Amino Acids (2011) 41:609–620
DOI 10.1007/s00726-011-0908-0

ORIGINAL ARTICLE

Formation of gels in the presence of metal ions

Nicola Castellucci · Giuseppe Falini · Gaetano Angelici · Claudia Tomasini

Received: 13 December 2010 / Accepted: 30 March 2011 / Published online: 13 April 2011

Abstract A small library of stereoisomeric pseudopeptides able to make gels in different solvents has been prepared and their attitude to make gels in the presence of several metal ions was evaluated. Four benzyl esters and four carboxylic acids, all containing a moiety of azelaic acid (a long chain dicarboxylic acid) coupled with four different pseudopeptide moieties sharing the same skeleton (a phenyl group one atom apart from the oxazolidin-2-one carboxylic group), were synthesized in solution, by standard coupling reaction. The tendency of these pseudopeptides to form gels was evaluated using the inversion test of 10 mM solutions of pure compounds and of stoichiometric mixtures of pseudopeptides and metal ions. To obtain additional information on the molecular association, the gel samples were left dry in the air to form xerogels that were further analyzed using SEM and XRD. The formation of gel containing Zn(II) or Cu(II) ions gave good results in term of incorporation of the metal ions, while the presence of Cu(I), Al(III) and Mg(II) gave less satisfactory results. This outcome is a first insight in the formation of stable LMWGs formed by stoichiometric mixtures of pseudopeptides and metal ions. Further studies will be carried out to develop similar compounds of pharmacological interest.

N. Castellucci · G. Falini (✉) · C. Tomasini (✉)
Dipartimento di Chimica "G. Ciamician",
Alma Mater Studiorum Università di Bologna,
Via Selmi 2, 40126 Bologna, Italy
e-mail: claudia.tomasini@unibo.it

G. Angelici
Department of Chemistry, University of Basel,
St. Johanns-Ring 19, 4056 Basel, Switzerland

Keywords Low molecular weight gelators · Pseudopeptides · Metal ions · Azelaic acid · Pseudoprolines

Abbreviations

D-Oxd	(4*R*,5*S*)-4-Carboxy-5-methyl oxazolidin-2-one
LMWG	Low molecular-weight gelator
L-Phe	L-Phenylalanine
SEM	Scanning electron microscopy
XRD	X-ray powder diffraction
CH_2Cl_2	Dichloromethane
AcOEt	Ethyl acetate
MeOH	Methanol
αMe-Phg	β^3-Homophenylglycine
β^3-hPhg	α-Methyl-phenylglycine
*O*Bn	*O*-Benzyl
D-Pro	D-Proline

Introduction

The term gel was coined in the 1860s (Graham 1861) to mean a wide variety of materials, easily identified by the simple "inversion test" (Raghavan and Cipriano 2005), where a test tube is inverted to ascertain whether the sample will flow under its own weight. A gel is assumed to be a sample that has a yield stress preventing it from flowing down the tube, while a sol is taken to be a sample that flows down the tube. The ability of compounds to gelate solvents relies on the balance between their tendency for self aggregation and their affinity for solvent molecules (Estroff and Hamilton 2004; Sangeetha and Maitra 2005; van Bommel et al. 2003; Yang and Xu 2007).

To understand the mechanism of gel formation, a gel can be broken down into a primary, secondary, and tertiary structure, much like a protein (Simmons et al. 2001; Aggeli et al. 2001). The primary structure (angstrom to nanometer scale) is determined by events at the molecular level that promote anisotropic aggregation in one or two dimensions of gelator molecules. To achieve gelation, there must be a balance between the tendency of the molecules to dissolve or to aggregate, and an intermolecular interaction of suitable strength is required for the formation of a gel (Zhu et al. 2010; Suzuki et al. 2010). Hydrogen bonding and π–π stacking interactions are the principle interactions involved in the aggregation of these molecules (Ajayaghosh and Praveen 2007; Ajayaghosh et al. 2008).

Traditional gel chemistry is dominated by polymers, but recently current interest is growing rapidly in "supramolecular" gels, composed of LMWGs and their complexes with metal ions and small anions (Piepenbrock et al. 2010; Terech and Weiss 1997). Self-assembled gels (also known as supramolecular or physical gels) comprised of LMWGs would theoretically be better suited to the field of biomaterials relative to polymer biomaterials because their scaffold of nanofiber networks are on the same order of magnitude as found in the extracellular matrix (ECM), thereby providing a pseudo in vivo environment for cell migration, growth, and differentiation. Furthermore, many LMWGs, being derived from biocompatible components and held together by noncovalent forces, degrade more-easily than the more prevalent polymer gels.

An extraordinary diverse range of compounds can act as LMWGs, but usually they have a long aliphatic chain, such as (*R*)-12-hydroxystearic acid (Huanga and Weiss 2007; Shibata et al. 2010) connected with a polar head, such as cholesteric acids (Hu et al. 2009; Bot et al. 2009). The tendency of the head to get organized into a three dimensional network enhances the probability to have the formation of a gel, that can be used in the chelation and delivery of metals for several applications, for instance in medicinal chemistry (Iwanaga et al. 2010; Morales et al. 2009) or in material sciences (Chatterjee et al. 2010; Li et al. 2010; Wicklein et al. 2009).

Several examples have been reported recently (Truong et al. 2011). Peptide amphiphiles (PAs) composed of a hydrophilic peptide head and a hydrophobic tail have evolved as biofunctional molecules that self-assemble into highly ordered nanostructures, leading to the formation of nanofibers, which can then undergo physical crosslinking to form three-dimensional networks to provide gel structures (Kim et al. 2009; Segers and Lee 2007). The self-assembled PA nanofiber gels have been extensively studied as potential biomaterials for tissue engineering scaffolds because of their ability to mimic the important properties of the natural ECM such as cell adhesion, proliferation, differentiation, and organization. Furthermore, organogels formed from *N*-stearoyl-L-alanine methyl ester in refined safflower oil can be used for the controlled delivery of rivastigmine, which is used to treat Alzheimer's disease (Vintiloiu et al. 2008).

Self-assembled gels are now showing significant promise in the field of localized drug delivery, as gels can easily fit into any shape that is required. For example, drugs mixed within a solution of LMWG, which forms a self-assembled gel on contact with bodily fluids such as blood (e.g., due to the resulting pH changes), could be delivered topically or by injection after tumor resection. On gelation, the gel theoretically would then be held in the cavity, thereby allowing the drugs to act locally (Ellis-Behnke et al. 2006).

A topic of great interest is nowadays the delivery of platinum(II)-based anticancer agents, as cisplatin, carboplatin and oxaliplatin, that are widely utilized in the clinic, although with numerous disadvantages, due to toxicity to "normal" tissues.

With the aim of circumventing unwanted side-effects, a great deal of research is being conducted in the areas of cancer-specific targeting, drug administration and drug delivery (Harper et al. 2010), that includes such technologies as liposomes, dendrimers, polymers and nanotubes, with all showing promise for the delivery of platinum compounds. The delivery of platinum(II)-based anticancer agents by means of self-assembled gels, made of stoichiometric amounts of LMWG and platinum(II) derivatives, could be a innovative answer against the high toxicity towards "normal" tissues.

The aim of this work is a first insight in the application of biocompatible gelators, derived from natural proteinogenic amino acids and fatty acids and able to chelate a series of metal ions. These compounds could be used in future to form self-assembled gels including platinum(II)-based anticancer agents or other compounds of pharmacological interest.

Results and discussion

A small library of stereoisomeric compounds, all containing a moiety of azelaic acid (a long chain dicarboxylic acid) coupled with different pseudopeptides was prepared. Azelaic acid was chosen after a screening among some long chain mono- and di-carboxylic acids: pseudopeptides derived from long chain mono-carboxylic acids (such as $C_5H_{11}COOH$ and $C_{11}H_{23}COOH$) do not form gels in any case. All these compounds contain the L-Phe-D-Oxd moiety. This skeleton is the minimal framework of a class of pseudopeptides, having the ability to self-organize (Angelici et al. 2008, 2009).

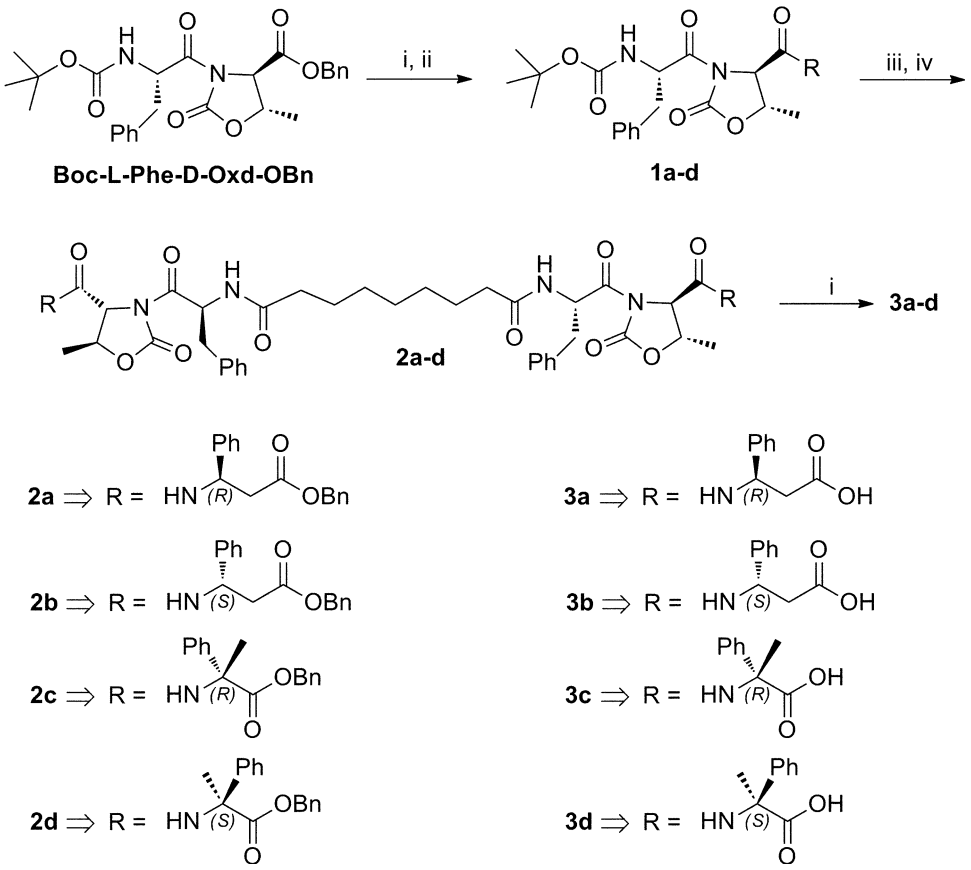

Scheme 1 Reagents and conditions (*i*) H_2, Pd/C MeOH, r,t. 2 h; (*ii*) α- or β-amino acid (1 equiv.), HBTU (1 equiv.), Et_3N (3 equiv.) dry CH_3CN, 40 min; (*iii*) TFA (18 equiv.), dry CH_2Cl_2, r. t., 4 h; (*iv*) azelaic acid (0.5 equiv.), HBTU (1 equiv.), Et_3N (3 equiv.) dry CH_3CN, 40 min

Scheme 1 reports the general formula of the eight compounds: they are four benzyl esters and four carboxylic acids. These compounds were synthesized in solution, by standard coupling reaction. Starting from Boc-L-Phe-D-Oxd-*O*Bn (Angelici et al. 2008), we prepared the four derivatives **1a–d** by replacing the *O*Bn moiety with four unusual amino acids: the two enantiomers of β^3-hPhg (Angelici et al. 2010) and the two enantiomers of αMe-Phg. Then we replaced the *N*-protection Boc moiety with azelaic acid to prepare derivatives **2a–d**. The four compounds were then deprotected by hydrogenolysis to give the free carboxy termini **3a–d**.

The tendency of these compounds to form gels was checked with the inversion test. To prepare gels, 6 mg of compounds **2a–d** or 5 mg of compounds **3a–d** were weighted out exactly in a test tube (8 mm wide), and then dissolved in the solvents reported in Table 1 (500 µl) to afford a 10 mM solution. As ultrasounds influence the aggregation properties of the molecules in the solvents (Choi et al. 2008, 2009; Isozaki et al. 2007), the tube was shaken for a few minutes by hand and then sonicated for 15 min at room temperature, then it was left standing still overnight before checking the gel formation.

The results of gelation tests of **2a–d** and **3a–d** are reported in Table 1. The tendency to form gels has been first checked for compounds **2a** and **2b**, in several solvents or mixtures of solvents. The best outcome was obtained with a 1:1 mixture of dichloromethane/ethyl acetate for **2a** and **2b** and with a 1:1 mixture of water and methanol for **3a** and **3b**. These mixtures of solvents were used to check if the more expensive compounds containing the αMe-Phg moiety (**2c**, **2d**, **3c** and **3d**) would form a gel. Unfortunately no gel formation was obtained in any case.

The gel–sol transition temperature (T_{gel}) gives important information on the thermal stability of the gels prepared in different ways (Takahashi et al. 1980; Yamanaka and Fujii 2009) and was measured by the ball-dropping method (see "Experimental"). Reversible gels, that reform after cooling down, are reported in entries 1, 5, 13 and 18.

The work was then continued only with compounds **2a**, **2b**, **3a** and **3b** to test their ability to generate a gelling status in the presence of several metal ions: Mg(II), Al(III), Zn(II), Cu(I) or Cu(II). The selection among the metal ion species was carried out trying to discriminate among two parameters: coordination chemistry and charge density. Mg(II) and Cu(II) have similar ionic radius (0.78 and 0.72 Å, respectively), but the former forms mainly octahedral coordination compounds, while the latter gives distorted octahedral coordination compounds that usually reorganize in tetrahedral or square planar geometries. Cu(I) ions and zinc ions

Table 1 Gelling status of the molecules **2a–d** and **3a–d**

Entry	Solvent	Compound	After sonication	After 2 h	M. p. (°C)
1	CH_2Cl_2/AcOEt 1:1	2a	SP	G	58[a]
2	$CHCl_3$/AcOEt 1:1	2a	PG	PG	–
3	AcOEt	2a	G	G	76[b]
4	Acetonitrile	2a	G	G	41[b]
5	CH_2Cl_2/AcOEt 1:1	2b	SP	G	80[a]
6	$CHCl_3$/AcOEt 1:1	2b	SP	SP	–
7	AcOEt	2b	PG	PG	–
8	Acetonitrile	2b	PG	PG	–
9	CH_2Cl_2/AcOEt 1:1	2c	SP	SP	–
10	CH_2Cl_2/AcOEt 1:1	2d	SP	SP	–
11	CH_2Cl_2	3a	PG	PG	–
12	H_2O	3a	SP	SP	–
13	MeOH/H_2O 1:1	3a	S	G	82[a]
14	*i*-PrOH/H_2O 1:1	3a	SP	PG	–
15	*i*-PrOH	3a	P	P	–
16	CH_2Cl_2	3b	P	P	–
17	H_2O	3b	P	P	–
18	MeOH/H_2O 1:1	3b	S	G	75[a]
19	*i*-PrOH/H_2O 1:1	3b	PG	PG	–
20	*i*-PrOH	3b	PG	G	80[b]
21	MeOH/H_2O 1:1	3c	S	S	–
22	MeOH/H_2O 1:1	3d	S	S	–

SP suspension, *G* gel, *PG* partial gel, *S* solution, *P* precipitate

[a] Reversible gel

[b] Non reversible gel

Table 2 Gelling status of the molecules **2a**, **2b**, **3a** and **3b** in the presence of metal ions

Molecule (solvent)	–[a]	CuBr	$CuBr_2$	$ZnBr_2$	$AlCl_3$	$MgBr_2$
2a (CH_2Cl_2/AcOEt, 1:1)	G (58)	PG	**G (62)**	G (50)	**G (75)**	SP
2b (CH_2Cl_2/AcOEt, 1:1)	G (80)	PG	G (60)	G (50)	PG	PG
3a (MeOH/H_2O, 1:1)	G (82)	S	G (68)	**G (92)**	PG	S
3b (MeOH/H_2O, 1:1)	G (75)	PG	SP	G (59)	SP	G (42)

The gel–sol transition temperature (T_{gel}) expressed in °C is reported in parenthesis. The gels that increase their T_{gel} (and consequently their thermal stability) in the presence of metal ions are in bold

SP suspension, *G* gel, *PG* partial gel, *S* solution

[a] Metal ions free gel

have different ionic radius (0.95 and 0.69 Å, respectively), but both preferentially form tetrahedral coordination compounds, however, Zn(II) have also a strong tendency to give octahedral geometries. Al(III) (ionic radius 0.45 Å) can give coordination compounds having tetrahedral and octahedral geometries, being the latter more common in the presence of charged ligands (Cotton et al. 1999). These metal ions have also different charge density: Al(III) > Zn(II) > Cu(II) ~ Mg(II) > Cu(I). The choice among the biological friendly chloride or bromide as counter anion was carried out in the view to give the gel a potential use of the gels to control the release of metal ions. As consequence, we paid a price in term of solubility in organic solvents.

Gels were prepared by suspension of an equimolecular amount of **2a** (or **2b**) and the inorganic salt, followed by sonication (see experimental). After 16 h, an homogeneous gel was formed. In the case of copper salts, the gel was pale green while in the other cases the gel was colorless. In the case of gels formed with **3a** (or **3b**) and the inorganic salt in methanol/water mixture, an homogeneous mixture was immediately formed and became a colorless gel after 16 h. The results of the gelation experiments of molecules **2a**, **2b**, **3a** or **3b** in the presence of metal ions are reported in Table 2.

While all these molecules formed gels in the reported conditions, they behave differently, in the presence of these five metal ions.

In the presence of Zn(II), they all formed gels, however, the strength of the gel was reduced, except for **3a**. On the contrary, Cu(I) prevents the formation of gels in any case,

as its presence in **2a**, **2b** and **3b** gave partial gels, while **3a** gave a suspension. A very different result was obtained with Cu(II): **2a**, **2b** and **3a** formed gels, while **3b** associated in a suspension. In the presence of Al(III) or Mg(II), the four compounds afforded very different results, as reported in Table 2. Only **2a** and **3b** form a gel in the presence of Al(III) and Mg(II), respectively. The former was stronger, and the latter weaker with respect to the corresponding metal ions free gels. In conclusion, among the tested molecules **2b** is the best gelator in the presence of metal ions, it always associates in a gel-like form, either gel or partial gel. **2a** failed to be in a gel-like form in the presence of Mg(II) only.

To obtain additional information on the molecular association, the gel samples were left to dry in the air to form xerogels that were further analyzed using SEM and XRD. The results of the SEM observations and of the XRD analyses are reported in Figs. 1, 2, 3.

The molecular assembly of **2a** in the xerogel is strongly affected by the presence of metal ions (Fig. 1). The metal ions free xerogel picture shows the presence of locally oriented long strips that cross on the large scale (Fig. 1 **2a**). Sometimes these strips merge laterally forming layers in which holes are present. The *scenario* of the xerogel changes in the presence of the metal ions: in the presence Cu(II) and Zn(II) the **2a** molecules form rope-like assemblies highly twisted (Fig. 1 **2_Zn(Cu)**), while in the presence of Al(III) **2a** mainly assembles forming a holed layered structure (Fig. 1 **2_Al**) that in some extent resembles what observed in the absence of metal ions. The XDR data (Fig. 1 right) show that **2a** is present in a crystalline form in the xerogel (as proved by the presence of several diffraction peaks) and that this status is not affected by the presence of metal ions, indeed the main diffraction peaks associated with the molecular structure do not change in relative intensity and angular position. This outcome indicates that metal ions do not influence the crystallinity and aggregation of the **2a** xerogels, therefore we can infer that the functional groups involved in the inter-molecular interactions responsible for the formation of the gel scaffold are not involved in the metal binding. In the XRD patterns from **2a_Cu(II)** and **2a_Al** xerogels, additional diffraction peaks associable to metal ion salts are detectable. Copper bromide is present in the **2a_Cu(II)** xerogel, while in the **2a_Al** xerogel the Al(III) compound(s) generating the diffraction peaks has not been identified. While Al(III) particles form aggregates that are SEM visible, copper bromide particles are not, suggesting that are finely dispersed in the xerogel structure (Fig. 2 **2a_Al, 2a_Cu(II)**). In contrast, in the **2a_Zn** xerogel XRD pattern only diffraction peaks due to **2a** appear, and no additional diffraction peaks were observed. Interestingly, the presence in the gel of metal ions compound crystalline particles (Cu(II) and Al(III)) increases its thermal stability (Table 2). Only the Zn(II) do not re-precipitate in the form of an inorganic crystalline material suggesting that they have a higher capability of interaction with the gel molecules or that form amorphous compounds. These observations suggest that the metal ions, although are not able to alter **2a** and **2b** molecular crystalline assembly (same XRD patterns), may affect the interactions among supra-molecular scaffold units, since the morphology of the xerogel is changed by their presence.

The SEM morphologies and the XRD patterns of the **2b** xerogels are reported in Fig. 2. **2b** associates forming a

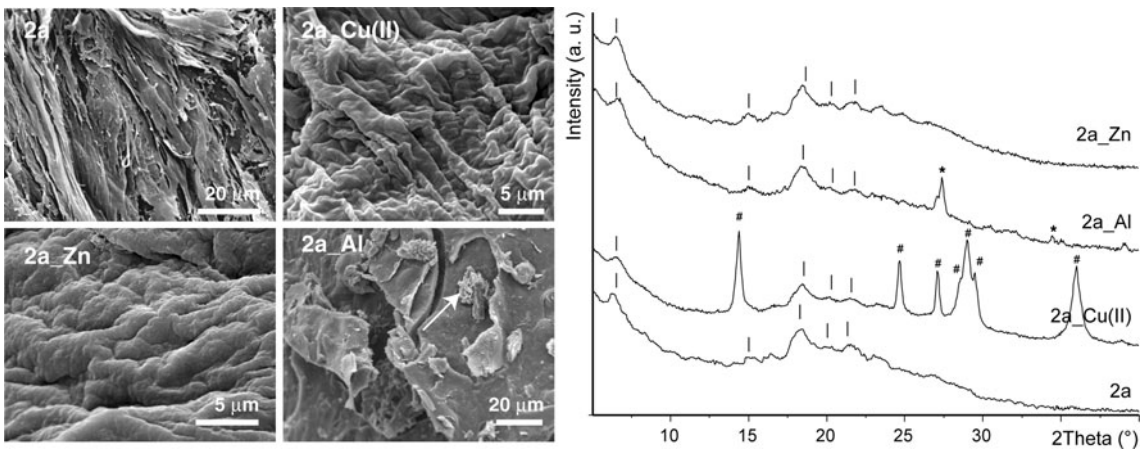

Fig. 1 The SEM images of the xerogels formed by the molecule **2a**: in the absence of metal ions (**2a**); the presence Cu(II) (**2a_Cu(II)**); in the presence of Zn(II) (**2a_Zn**) or in the presence of Al(III) (**2a_Al**) are shown on the *left*. The *arrow* in (**2a_Al**) indicates a crystalline aggregate made of an aluminium salt. On the *right* side, the corresponding X-ray powder diffraction patterns are reported. *Bars* indicate the diffraction peaks which could be associated with crystalline regions of **2a**. *Hash symbols* indicate the diffraction peaks that can be associated with crystalline $CuBr_2$, according to the powder diffraction file PDF 98-005-5875 (Simon and Oeckler 2000), *Asterisks* indicate the diffraction peaks associated with an Al containing compound that could not be identified (crystals from this unidentified compound are shown by the *arrow* in **2a_Al**)

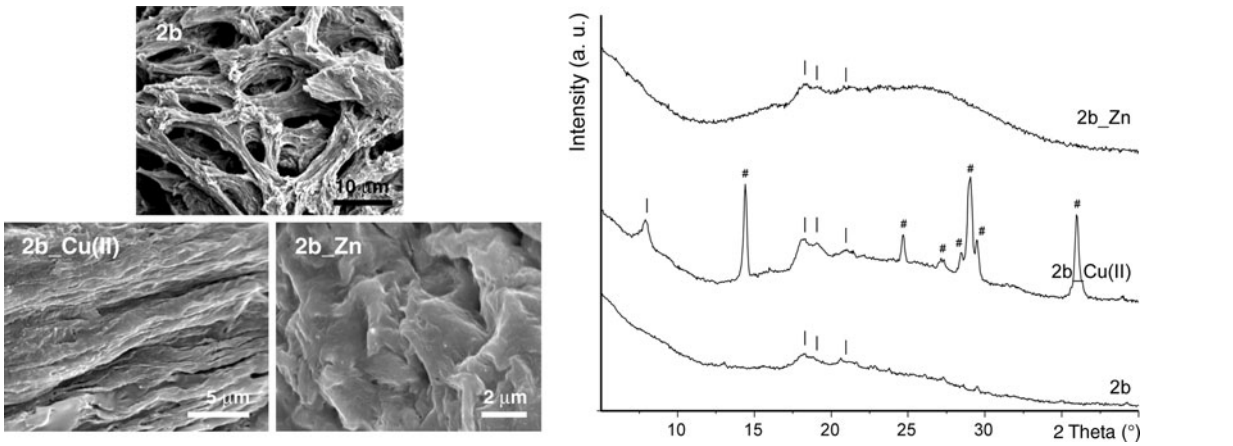

Fig. 2 The SEM images of the xerogels formed by: the molecule **2b** (**2b**) in the absence of metal ions; the molecule **2b** in the presence Cu(II) (**2b_Cu(II)**) or in the presence of Zn(II) (**2b_Zn**), are shown on the *left*. On the *right* side, the corresponding X-ray powder diffraction patterns are reported. *Bars* indicate the diffraction peaks which could be associated to crystalline regions of **2b**. *Hash symbols* indicate the diffraction peaks that can be associated to crystalline $CuBr_2$ according the powder diffraction file PDF 98-005-5875 (Simon and Oeckler 2000)

xerogel containing bundles of fibers that are branched, forming a complex web in which many holes are present. The presence of Cu(II) or Zn(II) changes the aggregation of **2b**, favouring the formation of highly twisted long rope-like aggregates, as previously observed for the **2a** xerogels obtained in similar conditions. This effect is not surprising, considering that the skeleton of **2a** and **2b** are very similar. The presence of Zn(II) seems to favour the merging of the rope-like structure giving a more compact material. The **2b_Cu(II)** xerogel hosts particles of crystalline copper bromide while the **2b_Zn** xerogel contains any Zn(II) crystalline compound. The crystallinity of **2b** in the xerogel increases in the presence of Cu(II), as revealed by the presence in the XRD pattern of more and more defined diffraction peaks.

Similar analyses were carried out on the xerogels obtained from **3a** and **3b** (Fig. 3). These compounds are very polar, as they contain a carboxylic group, and can form gels with mixtures of water and methanol. Besides its ability to form gels as a pure compound, **3a** retains its ability to form gel in the presence of Cu(II) and Zn(II) only. In the xerogel status, **3a** associates forming a porous structure in which no well defined structural motifs are observable. In the presence of Zn(II), **3a_Zn** xerogel structure makes a more compact material, as could be foreseen considering the high thermal stability of the **3a_Zn** gel (see Table 2). Also in this case we could suppose that the metal ions affects the way in which the molecular scaffolds make the gel. All the XRD patterns from **3a** xerogels show only one diffraction peak, indicating that the molecules are associated in a poor ordered way. Weak diffraction peaks due to copper(II) bromide are observable only in the XRD pattern from the **3a_Cu(II)** xerogel.

In the xerogel status, **3b** associates in porous structures similar to those formed by **3a,** also in the presence of Mg(II) or Zn(II). The **3b_Zn** xerogel is morphological similar to that of **3b** and makes entangled filaments that form a porous structure in which crystalline particles are embedded. On the contrary, the XRD pattern from **3b** xerogel is characterized by the presence of several diffraction peaks indicating a crystalline molecular aggregation, that are reduced by the presence of Zn(II). Finally, the XRD pattern from the **3b** xerogel hosting Mg(II) shows any diffraction peaks typical of the molecular packing, but shows only diffraction peaks due to unidentified mineral crystalline phases. In Table 3 a summary of the result of morphological and structural characterizations is reported.

The analysis of the results of the gelling experiments and the characterization of the xerogels can give some hints on the influence of the metal ions in the gelation process. Copper(I) ion has a negative effect on gel formation. This implies a weakening of the inter-molecular interactions making the gel. It may be related to its properties to give almost only complexes with tetrahedral coordination or to a strong change of the solvent features. Magnesium ions have also a negative role on the gelation capability of the molecules, as gel formation is inhibited except for **3b**, in which the gel thermal stability is reduced with respect to the metal free one. This may suggest a weakening of the interactions among the **3b** molecules due to Mg(II). These ions could interact with the molecules reducing their ability to form intermolecular bonds. Indeed, the periodic inter-molecular interactions (i.e. the crystallinity) in the **3b**

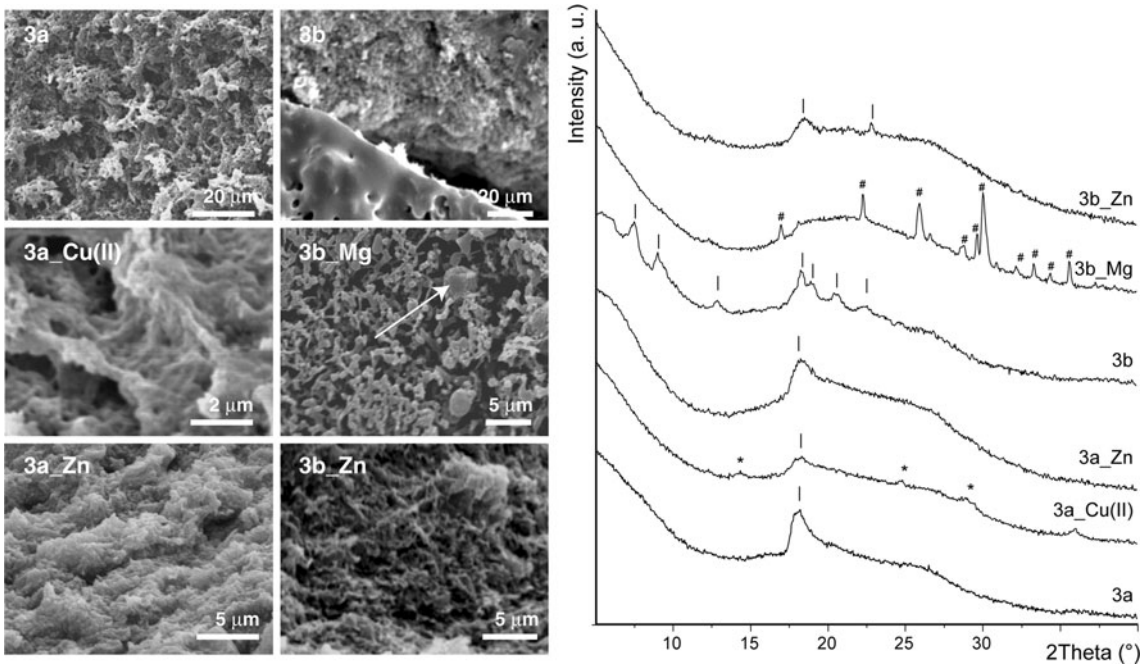

Fig. 3 The SEM images of the xerogels formed by: the molecule **3a** (**3a**) and the molecule **3b** (**3b**) in the absence of metal ions; the molecule **3a** in the presence Cu(II) ions (**3a_Cu(II)**) or in the presence of Zn ions (**3a_Zn**); the molecule **3b** in the presence of Mg ions (**3b_Mg**) or in the presence of Zn ions (**3b_Zn**), are shown on the *left*. The arrow in (**3b_Mg**) indicates a crystalline aggregate made of a magnesium salt. On the *right* side, the corresponding X-ray powder diffraction patterns are reported. *Bars* indicate the diffraction peaks which could be associated to crystalline regions of **3a** or **3b**. *Hash symbols* indicate the diffraction peaks that can be associated to crystalline $CuBr_2$ according the powder diffraction file PDF 98-005-5875 (Simon and Oeckler 2000). *Asterisks* indicates diffraction peaks that can not be univocally associated to specific crystalline forms

Table 3 Morphological and structural characterization of xerogels obtained from gels hosting metal ions

Molecule		[a]	CuBr	$CuBr_2$	$ZnBr_2$	$AlCl_3$	$MgBr_2$
2a	Morph.[c] polym. ()[d] min. ph. ()[e]	Strips phase 1	[b]	Rope like phase 1 (=) salt (no)	Rope like phase (=) –	Holed strips phase 1 (=) dif. salts (yes)	[b]
2b	Morph. polym. () min. ph. ()	Filaments phase 1	[b]	Rope like phase 1 (+) salt (no)	Rope like phase 1 (=)	[b]	[b]
3a	Morph. polym. () min. ph. ()	Spongy phase 1	[b]	Spongy phase 1 (−) salt (no)	Spongy phase 1 (=)	[b]	[b]
3b	Morph. polym. () min. ph. ()	Spongy phase 1	[b]	[b]	Spongy phase 1 (−−) –	[b]	Spongy amorphous dif. salts (yes)

In parenthesis, the presence (yes), or absence (no), of SEM observable mineral particles is indicated. In parenthesis is reported, the relative degree of crystallinity, evaluated from the intensity of the diffraction peaks, relative to the xerogel metal ions free: equal (=), higher (+), lower (−) or much lower (−−)

[a] Control experiment, xerogel obtained from metal free gel

[b] Gel did not form in the presence of the metal ions

[c] Morphological description of the xerogel

[d] Polymorphic phase of the peptide formed in the xerogel

[e] Observed mineral phase associated to the xerogel. Salt indicates the re-precipitation of the same salt dissolved in the gel

xerogel is reduced by the presence of magnesium ions. Al(III) inhibits the gel formation, except for the molecule **2a**. The **2a_Al** gel increases its thermal stability with respect to pure **2a** gel. This observation may suggest that Al(III) should strengthen the intermolecular interactions in the gel, although the crystallinity of the xerogel is not

affected. Al(III) being present as salt particles may act also as filler, improving the mechanical properties of the gel. Al(III) can form tetrahedral compounds other than octahedral ones, as Mg(II) does; this coordination flexibility may be involved in the alteration of the gel properties. The high charge density of Mg(II) may also have a role in destabilizing the gel structure.

Zn(II) does not inhibit the capability of the molecules to form gels. This means that the key molecular interaction forming the gel structure are not affected by the presence of Zn(II). These gels have thermal stability lower than the co-respective metal ion free **2a**, **2b** and **3b** gels. Only **3a** forms a gel with higher thermal stability in the presence of Zn(II). Interestingly, the xerogels obtained in the presence of Zn(II) do not contain any crystalline salt particles; this may be due to Zn(II)-molecules interactions that prevent the salt precipitation or the re-precipitation of Zn(II) salts in an amorphous form. These interactions, or the presence of small amorphous particles, may strengthen molecular entanglements, as occurs for **3a**, or weaken them, as occurs for **2a**, **2b** and **3b**.

Similar considerations may be applied to explain the effect of Cu(II) in the gel formation. However, in this case the xerogels obtained from the parent gels bearing Cu(II) always show the presence of particles of copper(II) bromide. Thus, it can be supposed that the interaction between copper(II) ions and the molecules is minimal or that is lost in the xerogel formation, although they are still trapped in the xerogel network.

Conclusions

In conclusion, a small library of LMWGs has been synthesized by coupling some pseudopeptides with azelaic acid, a long chain dicarboxylic acid. The ability to form gels in the presence of several solvents and of five metal ions, differing for their coordination chemistry and charge density has been analyzed.

Very good results have been obtained with Zn(II) and Cu(II) ions, that form gels in several conditions, while the formation of gels in the presence of Cu(I), Al(III) and Mg(II) affords less satisfactory results.

This outcome is a first insight in the formation of stable LMWGs obtained with stoichiometric mixtures of metal ions and pseudopeptides containing a moiety formed by phenyl group one atom apart from the oxazolidin-2-one carboxylic group. Further studies will be carried out to develop similar compounds of pharmacological interest. For instance self-assembled gels containing platinum(II)-based anticancer agents could furnish a innovative answer to the problem of delivery of these compounds, reducing their high toxicity towards "normal" tissues.

Experimental

The melting point of the compounds under investigation were determined in open capillaries and are uncorrected. High quality infrared spectra (64 scans) were obtained at 2 cm^{-1} resolution using a 1 mm NaCl solution cell and a FT-infrared spectrometer. All spectra were obtained in 3 mM solutions in dry CH_2Cl_2 at 297 K or as 1% solid mixture with dry KBr. All compounds were dried in vacuo and all the sample preparations were performed in a nitrogen atmosphere. Routine NMR spectra were recorded with spectrometers at 600, 400 or 300 MHz (^{1}H NMR) and at 150, 100 or 75 MHz (^{13}C NMR). The measurements were carried out in $CDCl_3$ and in DMSO-d_6. The proton signals were assigned by *g*COSY spectra. Chemical shifts are reported in δ values relative to the solvent ($CDCl_3$ or DMSO-d_6) peak.

General method for the preparation of compounds 1a–d

A solution of Boc-L-Phe-D-Oxd-OH (Angelici et al. 2009) (0.27 mmol, 0.10 g) and HBTU (0.3 mmol, 0.12 g) in dry acetonitrile (25 mL) was stirred under inert atmosphere for 10 min at room temperature. Then a mixture of the required α- or *β*- amino acid benzyl ester·TFA (see Fig. 1) (0.27 mmol, 0.10 g) and Et_3N (0.81 mmol, 0.12 mL) in dry acetonitrile (10 mL) was added at room temperature. The solution was stirred for 40 min under inert atmosphere, then acetonitrile was removed under reduced pressure and replaced with ethyl acetate. The mixture was washed with brine, 1 N aqueous HCl (3 × 30 mL) and with 5% aqueous $NaHCO_3$ (1 × 30 mL), dried over sodium sulphate and concentrated in vacuo. The product was obtained pure after silica gel chromatography (cyclohexane/ethyl acetate 8:2 as eluant) in 80–85% yield.

Boc-L-Phe-D-Oxd-(*R*)-*β*^{3}-*h*Phg-*O*Bn 1a (Angelici et al. 2010) **Boc-L-Phe-D-Oxd-(*S*)-*β*^{3}-*h*Phg-*O*Bn 1b** (Angelici et al. 2010) **Boc-L-Phe-D-Oxd-(*R*)-αMe-Phg-*O*Bn 1c** M.p. = 128°C; $[\alpha]_D^{20} = +88.9$ ($c = 1.1$, CH_2Cl_2); IR (CH_2Cl_2, 3 mM): *v* 3,437, 3,389, 3,336, 1,788, 1,737, 1,701, 1,678 cm^{-1}; IR (1% in dry KBr): *v* 3,390, 3,324, 1,783, 1,748, 1,716, 1,689 cm^{-1}; ^{1}H NMR (400 MHz, $CDCl_3$): δ 1.25 (d, 6H, $J = 6.3$ Hz), 1.55 (s, 9H), 1.97 (s, 3H), 2.84 (dd, 1H, $J = 8.0$, 13.2 Hz), 3.07 (dd, 1H, $J = 6.0$, 13.2 Hz), 4.29 (d, 1H $J = 3.6$ Hz), 4.43 (m, 1H), 4.91 (d, 1H, $J = 5.2$ Hz), 5.05 (AB, 2H, $J = 12.4$ Hz), 5.69 (m, 1H), 7.12–7.16 (m, 2H), 7.22–7.34 (m, 11H), 7.44–7.49 (m, 2H), 7.61 (s, 1H); ^{13}C NMR (75 MHz, $CDCl_3$): δ 21.4, 21.9, 28.4, 30.2, 38.0, 53.9, 62.7, 63.6, 67.8, 75.0, 80.1, 126.3, 127.7, 128.2, 128.5, 128.7, 128.9, 129.1, 129.7, 135.5, 136.2, 151.9, 173.3. Anal. calcd. for $C_{35}H_{39}N_3O_8$: C, 66.76; H, 6.24; N, 6.67; Found: C, 66.81; H, 6.20; N, 6.64.

Boc-L-Phe-D-Oxd-(*S*)-αMe-Phg-*O*Bn 1d M.p. = 196°C; $[\alpha]_D^{20} = +17.3$ ($c = 0.25$, CH_2Cl_2); IR (CH_2Cl_2, 3 mM): *v* 3,434, 3,385, 1,789, 1,737, 1,720, 1,703 cm^{-1}; IR (1% in dry KBr): *v* 3,389, 3,309, 1,768, 1,742, 1,718, 1,701, 1,687 cm^{-1}; NMR (400 MHz, $CDCl_3$): δ 1.26 (d, 6H, $J = 6.6$ Hz), 1.55 (s, 9H), 1.98 (s, 3H), 2.89 (m, 1H), 3.11 (m, 1H), 4.30 (m, 1H), 4.56 (m, 1H), 5.12 (AB, 2H, $J = 12.4$ Hz), 5.16 (bs, 1H), 5.71 (q, 1H, $J = 6.8$ Hz), 7.16–7.42 (m, 16H); ^{13}C NMR (75 MHz, $CDCl_3$): δ 21. 3, 28.5, 30.2, 54.3, 63.2, 68.0, 74.5, 126.4, 127.6, 128.3, 128.6, 128.8, 129.0, 129.8, 136.4, 151.8, 166.4, 173.8, 183.2. Anal. calcd. for $C_{35}H_{39}N_3O_8$: C, 66.76; H, 6.24; N, 6.67; Found: C, 66.73; H, 6.19; N, 6.70.

General method for the preparation of compounds 2a–d

A solution of fully protected di- or tripeptide (2 mmol) and TFA (36 mmol, 2.78 mL) in dry methylene chloride (20 mL) was stirred at room temperature for 4 h, then the volatiles were removed under reduced pressure and the corresponding amine salt was obtained pure in quantitative yield without further purification.

A solution of azelaic acid (0.98 g, 0.52 mmol) and HBTU (0.4 mg, 1.04 mmol) in dry acetonitrile (22 mL) was stirred under inert atmosphere for 10 min at room temperature. Then a mixture of the previously obtained amine salt (1.04 mmol) and Et_3N (3.2 mmol, 0.47 mL) in dry acetonitrile (15 mL) was added dropwise at room temperature. The solution was stirred for 40 min under inert atmosphere, then acetonitrile was removed under reduced pressure and replaced with ethyl acetate. The mixture was washed with brine, 1 N aqueous HCl (3 × 30 mL) and with 5% aqueous $NaHCO_3$ (1 × 30 mL), dried over sodium sulphate and concentrated in vacuo. The product was obtained pure after silica gel chromatography (DCM 100% → DCM/acetato di etile 80:20 as eluant).

$CH_2(C_3H_6CO$-L-Phe-D-Oxd-(*R*)-β^3-*h*Phg-*O*Bn$)_2$ 2a M.p. = 179°C; $[\alpha]_D^{20} = +44.0$ ($c = 1.1$, $CHCl_3$); IR (CH_2Cl_2, 3 mM): *v* 3,433, 3,323, 1,785, 1,735, 1,719, 1,672, 1,658 cm^{-1}; IR (1% in dry KBr): *v* 3,310, 3,298, 1,773, 1,734, 1,718, 1,653 cm^{-1}; ^1H NMR (400 MHz, $CDCl_3$): δ 1.09–1.58 (m, 16H), 1.85–2.05 (m, 4H), 2.85–3.21 (m, 8H), 4.11 (m, 2H), 4.39 (m, 1H), 4.62 (m, 1H), 5.05 (m, 2H), 5.13 (m 1H), 5.17 (s, 2H), 5.42 (m, 1H), 5.65 (m, 1H), 6.12 (m, 1H), 7.05–7.41 (m, 31H), 7.96 (m, 1H); ^{13}C NMR (50 MHz, $CDCl_3$): δ 20.8, 24.7, 28.3, 35.2, 36.5, 40.5, 41.1, 50.6, 53.3, 62.5, 66.5, 75.3, 82.1, 126.4, 127.4, 128.1, 128.5, 128.8, 129.2, 135.1, 135.6, 140.6, 143.5, 151.7, 167.1, 170.5, 172.9, 174.3. Anal. calcd. for $C_{69}H_{74}N_6O_{14}$: C, 68.41; H, 6.16; N, 6.94. Found: C, 68.47; H, 6.19; N, 6.91.

$CH_2(C_3H_6CO$-L-Phe-D-Oxd-(*S*)-β^3-*h*Phg-*O*Bn$)_2$ 2b M.p. = 129°C; $[\alpha]_D^{20} = +32.0$ ($c = 1.0$, CH_2Cl_2); IR (CH_2Cl_2, 3 mM): *v* 3,435, 3,319, 1,788, 1,735, 1,675, 1,655 cm^{-1}; IR (1% in KBr): *v* 3,411, 3,309, 3,088, 1,772, 1,732, 1,715, 1,650, 1,556, 1,531 cm^{-1}; ^1H NMR (400 MHz, $CDCl_3$): δ 1.08–1.52 (m, 16H), 1.92–2.15 (m, 4H), 2.81–2.99 (m, 6H), 3.18 (m, 2H), 4.12 (m, 2H), 4.39 (m, 1H), 4.58 (m, 1H), 5.05 (m, 2H), 5.13 (m 1H), 5.15 (s, 2H), 5.52 (m, 1H), 5.75 (m, 1H), 6.03 (m, 1H), 7.15–7.38 (m, 30H), 7.41 (d, 1H, $J = 6$ Hz), 7.85 (d, 1H, $J = 6.4$ Hz); ^{13}C NMR (50 MHz, $CDCl_3$): δ 21.0, 24.8, 28.5, 29.7, 35.3, 36.4, 40.8, 50.3, 53.2, 56.9, 62.5, 66.5, 75.2, 126.8, 127.5, 127.6, 128.2, 128.4, 128.7, 128.9, 129.2, 135.0, 135.7, 140.6, 151.0, 166.4, 170.1, 175.5, 174.3. Anal. calcd. for $C_{69}H_{74}N_6O_{14}$: C, 68.41; H, 6.16; N, 6.94. Found: C, 68.44; H, 6.17; N, 6.92.

$CH_2(C_3H_6CO$-L-Phe-D-Oxd-(*R*)-αMe-Phg-*O*Bn$)_2$ 2c M.p. = 76°C; $[\alpha]_D^{20} = +22.0$ ($c = 1.0$, $CHCl_3$); IR (CH_2Cl_2, 3 mM): *v* 3,343, 3,374, 3,366, 3,335, 1,787, 1,771, 1,738, 1,732, 1,683, 1,674 cm^{-1}; IR (1% in dry KBr): *v* 3,392, 3,370, 1,734, 1,701, 1,653 cm^{-1}; NMR (400 MHz, $CDCl_3$): δ 0.98–1.44 (m, 16H), 1.88–2.05 (m, 4H), 1.96 (s, 6H), 2.92 (m, 2H), 3.17 (m, 2H), 4.24 (m, 2H), 4.41 (m, 2H), 5.12 (AB, 4H, $J = 12.4$ Hz), 5.28 (m, 2H), 5.78 (bs, 1H), 6.10 (bs, 1H), 7.05–7.37 (m, 29H), 7.44 (m, 2H), 7.81 (m, 1H); ^{13}C NMR (50 MHz, $CDCl_3$): δ 21.0, 24.6, 24.7, 28.3, 28.4, 28.5, 35.3, 36.8, 53.0, 62.4, 62.7, 67.5, 74.4, 126.3, 127.3, 127.4, 128.1, 128.2, 128.4, 128.7, 129.3, 135.2, 139.4, 151.6, 166.6, 171.7, 173.0, 173.6. Anal. calcd. for $C_{69}H_{74}N_6O_{14}$: C, 68.41; H, 6.16; N, 6.94. Found: C, 68.37; H, 6.19; N, 6.99.

$CH_2(C_3H_6CO$-L-Phe-D-Oxd-(*S*)-αMe-Phg-*O*Bn$)_2$ 2d M.p. = 150°C; $[\alpha]_D^{20} = +92.0$ ($c = 1$, $CHCl_3$); IR (CH_2Cl_2, 3 mM): *v* 3,433, 3,385, 3,323, 3,304, 1,787, 1,737, 1,714, 1,677 cm^{-1}; IR (1% in KBr): *v* 3,422, 3,327, 3,284, 1,781, 1,749, 1,706, 1,684, 1653, 1642 cm^{-1}; ^1H NMR (400 MHz, $CDCl_3$): δ 0.88–1.41 (m, 16H), 1.65–2.02 (m, 4H), 1.96 (s, 6H), 2.94 (m, 2H), 3.18 (m, 2H), 4.24 (m, 2H), 4.42 (m, 2H), 5.08 (AB, 4H, $J = 12.0$ Hz), 5.28 (m, 2H), 5.71 (bs, 2H), 6.05 (bs, 2H), 7.05–7.35 (m, 30H), 7.40 (bs, 1H), 7.78 (s, 1H); ^{13}C NMR (100 MHz, $CDCl_3$): δ 14.1, 20.8, 21.0, 21.8, 24.5, 28.5, 29.6, 35.2, 36.7, 53.0, 53.4, 60.3, 62.2, 63.0, 67.3, 74.6, 81.4, 126.1, 127.3, 127.9, 128.0, 128.1, 128.3, 128.7, 129.2, 135.4, 151.6, 166.9, 171.6, 173.4. Anal. calcd. for $C_{69}H_{74}N_6O_{14}$: C, 68.41; H, 6.16; N, 6.94. Found: C, 68.45; H, 6.20; N, 6.91.

General method for the preparation of compounds 3a–d

Compound **1a–e** (1 mmol) was dissolved in MeOH (35 mL) under nitrogen. C/Pd (50 mg, 10% w/w) was

added under nitrogen. A vacuum was created inside the flask using the vacuum line. The flask was then filled with hydrogen using a balloon (1 atm). The solution was stirred for 2 h under a hydrogen atmosphere. The product was obtained pure after filtration through a Celite pad using ethyl acetate and concentration in vacuo.

CH_2(C_3H_6CO-L-Phe-D-Oxd-(*R*)-β^3-*h*Phg-OH)$_2$ 3a M.p. = 140°C; $[\alpha]_D^{20} = +29.0$ ($c = 1.0$, MeOH); ^{1}H NMR (CD_3OD, 400 MHz): δ 0.82–1.59 (m, 16H), 2.03–2.35 (m, 4H), 2.61–2.98 (m, 4H), 3.15–3.40 (m, 4H), 4.41 (M, 2H), 4.48–4.90 (m, 4H), 5.38 (m, 2H), 5.95 (m, 2H), 7.05–7.43 (m, 20H); ^{13}C NMR (CD_3OD, 100 MHz): δ 19.7, 20.0, 25.4, 28.3, 28.4, 29.1, 35.4, 37.2, 40.3, 46.5, 48.1, 50.7, 63.1, 75.6, 126.1, 128.3, 128.4, 137.8, 142.0, 153.6, 168.2, 172.3, 173.0, 174.4. Anal. calcd. for $C_{55}H_{62}N_6O_{14}$: C, 64.07; H, 6.06; N, 8.15. Found: C, 64.15; H, 6.04; N, 8.14.

CH_2(C_3H_6CO-L-Phe-D-Oxd-(*S*)-β^3-*h*Phg-OH)$_2$ 3b M.p. = 117°C; $[\alpha]_D^{20} = -31.7$ ($c = 1.3$, MeOH); ^{1}H NMR (CD_3OD, 400 MHz): δ 1.05–1.59 (m, 16H), 2.03–2.25 (m, 4H), 2.71–2.94 (m, 4H), 3.10–3.35 (m, 4H), 4.41 (M, 2H), 4.51–4.78 (m, 4H), 5.38 (m, 2H), 5.98 (m, 2H), 7.05–7.43 (m, 20H); ^{13}C NMR (CD_3OD, 100 MHz): δ 19.6, 25.5, 28.7, 35.3, 37.6, 40.7, 50.4, 53.0, 60.8, 63.1, 65.9, 75.2, 126.4, 126.8, 127.3, 128.2, 128.4, 129.4, 136.7, 143.6, 160.3, 174.8. Anal. calcd. for $C_{55}H_{62}N_6O_{14}$: C, 64.07; H, 6.06; N, 8.15. Found: C, 64.00; H, 6.04; N, 8.19.

CH_2(C_3H_6CO-L-Phe-D-Oxd-(*R*)-αMe-Phg-OH)$_2$ 3c M.p. = 98°C; $[\alpha]_D^{20} = +52.0$ ($c = 0.6$, MeOH); ^{1}H NMR (CD_3OD, 400 MHz): δ 0.90–1.61 (m, 16H), 1.92–2.10 (m, 4H), 1.97 (s, 6H), 2.92 (m, 2H), 3.16 (m, 2H), 3.60–3.95 (m, 2H),4.42–4.60 (m, 4H), 5.95 (m, 2H), 7.05–7.60 (m, 20H); ^{13}C NMR (CD_3OD, 100 MHz): δ 19.4, 19.7, 21.3, 22.3, 25.3, 28.4, 28.6, 30.0, 35.1, 36.9, 52.8, 53.7, 61.7, 62.9, 74.6, 77.0, 125.7, 125.9, 126.5, 127.0, 127.1, 127.7, 127.8, 128.0, 128.7, 129.1, 136.5, 136.8, 152.3, 167.5, 169.5, 172.3, 174.8. Anal. calcd. for $C_{55}H_{62}N_6O_{14}$: C, 64.07; H, 6.06; N, 8.15. Found: C, 64.11; H, 6.01; N, 8.12.

CH_2(C_3H_6CO-L-Phe-D-Oxd-(*R*)-αMe-Phg-OH)$_2$ 3d M.p. = 115°C; $[\alpha]_D^{20} = -4.5$ ($c = 1.2$, MeOH); ^{1}H NMR (CD_3OD, 400 MHz): δ 90–1.70 (m, 16H), 1.85 (s, 6H), 1.90–2.25 (m, 4H), 2.88 (m, 2H), 3.95 (m, 1H), 4.20 (m, 1H), 4.48–4.65 (m, 4H), 5.98 (m, 2H), 7.11–7.58 (m, 20H); ^{13}C NMR (CD_3OD, 100 MHz): δ 19.4, 19.7, 22.0, 25.4, 28.4, 28.6, 29.3, 35.2, 37.4, 52.8, 62.6, 74.4, 125.9, 126.1, 126.2, 127.2, 127.9, 128.0, 128.2, 128.7, 129.1, 136.6, 140.6, 152.4, 167.7, 168.0, 172.2, 174.4. Anal. calcd. for $C_{55}H_{62}N_6O_{14}$: C, 64.07; H, 6.06; N, 8.15. Found: C, 64.11; H, 6.10; N, 8.12.

Conditions for the gel formation

Compounds 2a–d (6 mg, 5 μmol) or 3a–d (5 mg, 5 μmol) and the solvent reported in Table 1 (500 μl) were placed in a test tube (8 mm wide). In some cases, the mixture was sonicated to speed dissolution, by breaking intermolecular interactions.

The tube was shaken for a few minutes by hand and then sonicated for 15 min at room temperature, then let stand for 16 h for the gel formation. The xerogel was obtained, after solvent evaporation at room temperature.

Conditions for the gel formation with inorganic salts

Compounds **2a–b** (6 mg, 5 μmol) or **3a–b** (5 mg, 5 μmol) and the solvent reported in Table 2 (500 μl) were placed in a test tube (8 mm wide) together with 1 equivalent of the inorganic salt. In the case of the organic solvent, the organic salt remained as a precipitate.

The tube was shaken for a few minutes by hand and then sonicated for 15 min at room temperature, then let stand for 16 h for the gel formation. When the gel was formed, no more precipitate was present in the test tube. The xerogel was obtained, after solvent evaporation at room temperature.

Conditions for T_{gel} determination

The gel–sol transition temperature (T_{gel}) was determined by heating some test tubes (diameter: 8 mm) containing the gel and a glass ball (diameter: 5 mm, weight: 165 mg) on the top of it. When the gel is formed, the ball floats on it. The T_{gel} is the temperature at which the gel becomes sol and, as a consequence, the ball falls down.

Microscopy

The precipitates were systematically observed by optical microscopy (OM) and scanning electron microscopy (SEM). The OM images were collected using an optical microscope equipped with a CCD camera. Samples SEM images were collected on glass cover slip after coating with gold and observed using a scanning electron microscope. The images were recorded using a CCD digital camera.

X-ray powder diffraction analysis

Powder X-ray diffraction patterns were collected using a powder diffractometer using Cu Kα radiation generated at 40 kV and 40 mA. The instrument was configured with a 1/16° divergence and 1/16° antiscattering slits. A standard quartz sample holder 1 mm deep, 20 mm high and 15 mm wide was used. The diffraction patterns were collected

within the 2θ range from 5° to 40° with a step size ($\Delta\ 2\theta$) of 0.02° and a counting time of 60 s.

Acknowledgments CT is grateful to Ministero dell'Università e della Ricerca Scientifica (PRIN 2008), Università di Bologna (Funds for selected topics) and to Fondazione del Monte di Bologna e di Ravenna for financial support. GF thanks the Consorzio Inter-Universitario di Ricerca della Chimica dei Metalli nei Sistemi Biologici for financial support.

Conflict of interest The authors declare that they have no conflict of interest.

References

Aggeli A, Nyrkova IA, Bell M, Harding R, Carrick L, McLeish TCB, Semenov AN, Boden N (2001) Hierarchical self-assembly of chiral rod-like molecules as a model for peptide b-sheet tapes, ribbons, fibrils, and fibers. Proc Natl Acad Sci USA 98(21):11857–11862

Ajayaghosh A, Praveen VK (2007) π-Organogels of self-assembled *p*-Phenylenevinylenes: soft materials with distinct size, shape, and functions. Acc Chem Res 40(8):644–656

Ajayaghosh A, Praveen VK, Vijayakumar C (2008) Organogels as scaffolds for excitation energy transfer and light harvesting. Chem Soc Rev 37(1):109–122

Angelici G, Falini G, Hofmann HJ, Huster D, Monari M, Tomasini C (2008) A fiber-like peptide material stabilized by single intermolecular hydrogen bonds. Angew Chem Int Ed 47(42):8075–8078

Angelici G, Falini G, Hofmann H-J, Huster D, Monari M, Tomasini C (2009) Nanofibers from oxazolidi-2-one containing hybrid foldamers: what is the right molecular size? Chem Eur J 15(32):8037–8048

Angelici G, Castellucci N, Falini G, Huster D, Monari M, Tomasini C (2010) Pseudopeptides designed to form supramolecular helixes: the role of the stereogenic centers. Cryst Growth Des 10(2):923–929

Bot A, den Adel R, Roijers EC, Regkos C (2009) Effect of sterol type on structure of tubules in sterol + γ-oryzanol-based organogels. Food Biophys 4:266–272

Chatterjee J, Liu T, Wang B, Zheng JP (2010) Highly conductive PVA organogel electrolytes for applications of lithium batteries and electrochemical capacitors. Solid State Ion 181(11–12):531–535

Choi YY, Joo MK, Sohn YS, Jeong B (2008) Significance of secondary structure in nanostructure formation and thermosensitivity of polypeptide block copolymers. Soft Matter 4(12):2383–2387

Choi YY, Jeong Y, Joo MK, Jeong B (2009) Reverse thermal organogelation of poly(ethylene glycol)-polypeptide diblock copolymers in chloroform. Macromol Biosci 9(9):869–874

Cotton FA, Wilkinson G, Murillo CA, Bochmann M (1999) Advanced inorganic chemistry, 6th edn. Wiley, New York

Ellis-Behnke RG, Liang YX, Tay DKC, Kau PWF, Schneider GE, Zhang S, Wu W, So KF (2006) Nano hemostat solution: immediate hemostasis at the nanoscale. Nanomedicine 2(4):207–215

Estroff LA, Hamilton AD (2004) Water gelation by small organic molecules. Chem Rev 104(3):1201–1217

Graham T (1861) Liquid diffusion applied to analysis. Philos Trans R Soc 151:183–224

Harper BW, Krause-Heuer AM, Grant MP, Manohar M, Garbutcheon-Singh KB, Aldrich-Wright JR (2010) Advances in platinum chemotherapeutics. Chem Eur J 16(24):7064–7077

Hu J, Zhang M, Ju Y (2009) A simple oleanlic acid derivative as potent organogelator. Soft Matter 5:4971–4974

Huanga X, Weiss RG (2007) Molecular organogels of the sodium salt of (*R*)-12-hydroxystearic acid and their templated syntheses of inorganic oxides. Tetrahedron 63(31):7375–7385

Isozaki K, Takaya H, Naota T (2007) Ultrasound-induced gelation of organic fluids with metallated peptides. Angew Chem Int Ed 46(16):2855–2857

Iwanaga K, Sumizawa T, Miyazaki M, Kakemi M (2010) Characterization of organogel as a novel oral controlled release formulation for lipophilic compounds. Int J Pharm 388(1–2):123–128

Kim JK, Anderson J, Jun HW, Repka MA, Jo S (2009) Self-assembling peptide amphiphile-based nanofiber gel for bioresponsive cisplatin delivery. Mol Pharm 6(3):978–985

Li JL, Yuan B, Liu XY, Xu HY (2010) Microengineering of supramolecular soft materials by design of the crystalline fiber networks. Cryst Growth Des 10(6):2699–2706

Morales ME, Gallardo V, Clares B (2009) Study and description of hydrogels and organogels as vehicles for cosmetic active ingredients. J Cosmet Sci 60(6):627–636

Piepenbrock MOM, Lloyd GO, Clarke N, Steed JW (2010) Metal and anion-binding supramolecular gels. Chem Rev 110(4):1960–2004

Raghavan SR, Cipriano BH (2005) Gel formation: phase diagrams using tabletop rheology and calorimetry. In: Weiss RG, Terech P Springer, Amsterdam, p 233

Sangeetha NM, Maitra U (2005) Supramolecular gels: functions and uses. Chem Soc Rev 34(10):821–836

Segers VFM, Lee RT (2007) Local delivery of proteins and the use of self-assembling peptides. Drug Discov Today 12(13/14):561–568

Shibata M, Teramoto N, Kaneko K (2010) Molecular composites composed of castor oil-modified poly(e-caprolactone) and self-assembled hydroxystearic acid fibers. J Pol Sci Part B Pol Phys 48(12):1281–1289

Simmons BA, Taylor CE, Landis FA, John VT, McPherson GL, Schwartz DK, Moore R (2001) Microstructure determination of AOT + Phenol organogels utilizing small-angle X-ray scattering and atomic force microscopy. J Am Chem Soc 123(10):2414–2421

Simon A, Oeckler O (2000) Redetermination of the crystal structure of copper dibromide, $CuBr_2$. Z Kristallogr 215(1):13–21

Suzuki M, Abe T, Hanabusa K (2010) Low-molecular-weight gelators based on N^{α}-acetyl-N^{ε}-dodecyl-L-lysine and their amphiphilic gelation properties. J Coll Interface Sci 341(1):69–74

Takahashi K, Sakai M, Kato T (1980) Melting temperature of thermally reversible gel. VI. Effect of branching on the Sol–Gel transition of polyethylene gels. Polymer J 12(5):335–341

Terech P, Weiss RG (1997) Low molecular mass gelators of organic liquids and the properties of their gels. Chem Rev 97(8):3133–3159

Truong WT, Su Y, Meijer JT, Thordarson P, Braet F (2011) Self-assembled gels for biomedical applications. Chem Asian J 6(1):30–42

van Bommel KJC, Friggeri A, Shinkai S (2003) Organic templates for the generation of inorganic materials. Angew Chem Int Ed 42(9):980–999

Vintiloiu A, Lafleur M, Bastiat G, Leroux JC (2008) In situ-forming oleogel implant for rivastigmine delivery. Pharm Res 25(4):845–852

Wicklein A, Ghosh S, Sommer M, Wuerthner F, Thelakkat M (2009) Self-assembly of semiconductor organogelator nanowires for photoinduced charge separation. ACS Nano 3(5):1107–1114

Yamanaka M, Fujii H (2009) Chloroalkane gel formations by tris–urea low molecular weight gelator under various conditions. J Org Chem 74(15):5390–5394

Yang Z, Xu B (2007) Supramolecular hydrogels based on biofunctional nanofibers of self-assembled small molecules. J Mater Chem 17(23):2385–2393

Zhu PL, Yan XH, Su Y, Yang Y, Li JB (2010) Solvent-induced structural transition of self-assembled dipeptide: from organogels to microcrystals. Chem Eur J 16(10):3176–3183